IOSR Journal of Electrical and Electronics Engineering (IOSR-JEEE)
e-ISSN: 2278-1676,p-ISSN: 2320-3331, Volume 11, Issue 1 Ver. I (Jan – Feb. 2016), PP 91-98
www.iosrjournals.org

Immune Optimization of Path Planning for Coal Mine Rescue Robot

Peng Li, Hua Zhu*
(School of Mechanical and Electronic Engineering,China University of Mining and Technology, Xuzhou,China)

Abstract : *In order to further improve the ability of global path planning of coal mine rescue robot in the complex environment, a bacterial foraging algorithm-based polyclonal selection algorithm (BFA-PSA) is proposed. In order to verify the superiority of the BFA-PSA, the proposed algorithm is tested by traveling salesman problem (TSP) and compared with genetic algorithm (GA) and clonal selection algorithm (CSA). Finally, on the basis of grid environment model, the BFA-PSA is used in the optimization of path planning for coal mine rescue robot. The optimization results of the TSP show that the searching ability and efficiency of the BFA-PSA are improved. And the optimization results of path planning for coal mine rescue robot in the grid environment model show the better robustness and validity of the BFA-PSA.*

Keywords : *Path planning; Bacteria foraging; Clonal selection; TSP; Grid method*

I. Introduction

With the improvement of industrial level, demand for coal of China is growing[1].Many serious coal mine accidents often occurred due to poor geological conditions in coal mines, containing gas, the low mechanized level of coal mining equipment, non-standard operation of workers, etc. After the gas explosion of coal mine, the environment of coal mine is extremely unstable and the secondary explosion occurs possibly. It is difficult for the rescue workers to arrive at the scene and carry out the rescue work at first time[2]. Therefore, countries all over the world hasten the development of coal mine rescue robot in order to ensure the implementation of the coal mine rescue work. Abroad, coal mine rescue robots mainly include Simbot[3], Groundhog[4], Ratler[5], etc. While in China, coal mine rescue robots mainly include a series of CUMT[6-9].Coal mine rescue request that rescue workers or equipment must arrive at the scene of the accident at first time in order to save more time[10].There are multiple paths for a coal mine rescue robot to choose, and people pay more attention on how to make the robot avoid obstacles, and choose the shortest one.

Path planning is the key technology of mobile robot navigation [11], and it is usually divided into conventional way and intelligent way. The conventional way includes artificial potential field[12], grid method[13], etc. The artificial potential field has a small amount of calculation, a good real-time performance, and a simple model,however, it also appears a shortage of the local minimum. The grid method requires an appropriate work area. The intelligent way includes neural network[14], fuzzy logic[15], genetic algorithm[16], etc. It is difficult for the neural network to obtain sufficient sample data. Although the fuzzy logic overcomes the local minimum, its experience is incomplete. Because of global optimization ability, the genetic algorithm is used in path planning in these years, but it has a slow convergence speed. Global path planning based on intelligent algorithm is getting more and more attention, but the general path planning intelligent algorithms based on grid model for robot is easy to fall into local minimum, and their optimization ability remains to be further improved. In order to further improve the ability of global path planning for coal mine rescue robot in complex environment, a bacterial foraging algorithm-based polyclonal selection algorithm is proposed in this paper, and it is successfully used in path planning of coal mine rescue robot.

II. Clonal selection algorithm

In 1957, Burnet put forward the clonal selection algorithm (CSA)[17]. With learning, recollecting and pattern recognition function, this algorithm provides many enlightenments and references for solving the engineering problems.

In general, taking $x=[x_1\ x_2 \cdots x_n]$ as a variable, this paper considers the following optimization model:

$$\max \quad f(x) = \max \quad f(e^{-1}(a)) \qquad (1)$$

Where, f is the objective function, a is the antibody coding of x, $e^{-1}(\cdot)$ is the decoding style, namely, $x=e^{-1}(a)$.

*** Corresponding author.** E-mail: zhuhua83591917@163.com

2.1 Clonal operation T_c^C

Known, $A(k)=[a_1(k)\ a_2(k)\ \cdots\ a_n(k)]^T$. Where, $A(k)$is the antibody population. The clone operation is defined as:

$$A'(k) = T_c^C(A(k)) = [A_1'(k)\ \ A_2'(k)]\ \cdots\ A_n'(k)]^T \tag{2}$$

$$\forall i \in [1,n],\quad A_i'(k) = T_c^C(a_i(k)) = I_i \times a_i(k) = [a_{i1}'(k)\ \ a_{i2}'(k)\ \cdots\ a_{id_i}'(k)]^T .$$

Where, I_i is n-dimensional vector, and its element value is 1. $\forall j \in [1, d_i]$, $a_{ij}(k) = a_i(k)$.In particular, taking d_i:

$$d_i = Int\left(N_c \times \frac{f(e^{-1}(a_i(k)))}{\sum_{j=1}^{n} f(e^{-1}(a_j(k)))} \right) \tag{3}$$

Where, $Int(\cdot)$ is the top integral function in order to ensure I_i be not a null vector. N_c is the clone scale value, and $N_c > n$.

2.2 Immune gene operation T_g^C

Immune gene operation includes crossover and mutation, the monoclonal selection algorithm only includes mutation operation, while the polyclonal selection algorithm includes crossover and mutation operation. In this paper, we make use of polyclonal selection algorithm. p_c is the probability of crossover operation, and p_m is the probability of mutation operation.

2.2.1 Crossover operation

$A'(k)$ comes from clonal operation, and it becomes to $A^c(k)$ by crossover operation in the probability of p_c. The operation can be described as:

$$A^c(k) = T_{gc}^C(A'(k)) \tag{4}$$

$$\forall i = [1,n],\quad \forall j = [1,d_i],\quad a_{ij}^c(k) = a'_{i_{c1}j_{c1}}(k)\,\Delta\, a'_{i_{c2}j_{c2}}(k),\quad a'_{i_{c1}j_{c1}}(k) \in A'(k),\quad a'_{i_{c2}j_{c2}}(k) \in A'(k),$$

$$i_{c1} = Int(rand \times n),\quad j_{c1} = Int(rand \times d_i),\quad i_{c2} = Int(rand \times n),\quad j_{c2} = Int(rand \times d_i).$$

Where $a\Delta b$ shows that a and b take crossover operation in the probability of p_c.

2.2.2 Mutation operation

$A^c(k)$ comes from crossover operation, and it becomes to $A^m(k)$ by mutation operation in the probability of p_m. The operation can be described as:

$$A^m(k) = T_{gm}^C(A^c(k)) \tag{5}$$

$$\forall i = [1,n],\ \forall j = [1,d_i],\ a_{ij}^m(k) = \tilde{a}_{ij}^c(k)^x,\ a_{ij}^c(k) = A^c(k),\ bits = Int(rand \times l).$$

Where, l is the encoding length of a^c_{ij}(k), $\tilde{a}_{ij}^c(k)^x$ shows that reversing the x bits of a^c_{ij}(k) in the probability of p_m.Given the above, A ‘’ (k) can be described as:

$$A''(k) = T_g^C(A'(k)) = T_{gm}^C(T_{gc}^C(A'(k))) = [A_1''(k)\ \ A_2''(k)\cdots\ A_n''(k)]^T \tag{6}$$

2.3 Clonal selection operation T_s^C

The clonal selection operation picks out the best individual which is effected by clonal operation and immune gene operation to form a new population. The operation can be described as:

$$A(k+1) = T_s^C(A''(k)) = [a_1(k+1)\ \ a_2(k+1)\cdots\ a_n(k+1)] \tag{7}$$

$$\forall i = [1,n],\ \forall j = [1,d_i],\ a_i(k+1) = \max\ f(e^{-1}(a_{ij}''(k) \cup a_i(k))) .$$

The clonal selection algorithm is a new global optimization search intelligent algorithm. This algorithm has both global search and local search, and it can maintain the diversity of the population. But at the same time, this algorithm has a slow convergence speed and a large amount of calculation. In order to solve the convergence phenomenon which often occurs in the basic PSA causing the algorithm to fall into local minima at the late of the optimization, the bacterial foraging algorithm is introduced into the polyclonal selection algorithm.

III. Bacterial Foraging Algorithm

In 2002, K.M. Passino put forward the bacterial foraging algorithm (BFA) [18]which simulates the foraging behavior of Escherichia coil in human intestine. This algorithm can search in parallel, and it is easy to jump out from local minima. The bacterial foraging algorithm includes chemotaxis operator , reproduction operator and elimination-dispersal operator.

In general, taking $x=[x_1\ x_2\ \cdots x_n]^T$ as a variable, this paper considers the following optimization model:

$$\min\ f(x) = \min\ f(e^{-1}(b)) \tag{8}$$

Where, f is the objective function, b is the antibody coding of x, $e^{-1}(\cdot)$ is the decoding style, namely, $x=e^{-1}(a)$.

3.1 Chemotaxis operator T_c^B

Known, $B(k)=[b_1(k)\ b_2(k)\ \cdots\ b_n(k)]^T$. Where, $B(k)$ is the antibody population. The chemotaxis operator is defined as:

$$B'(k) = T_c^B(B(k)) = [b_1'(k)\ \ b_2'(k)\cdots\ b_n'(k)]^T \tag{9}$$

$\forall i \in [1,n]$, $b_i'(k) = T_c^B(b_i(k))$, $b_i(k) = b_i^k(j,m,l)$, $b_i'(k) = b_i'^k(j+1,m,l)$, namely,

$$b_i'^k(j+1,m,l) = b_i^k(j+1,m,l) + rand \times step \times \varphi_i(j,m,l) \tag{10}$$

$$\varphi_i(j,m,l) = \frac{b_i^k(j,m,l) - b_{rand}^k(j,m,l)}{\left\| b_i^k(j,m,l) - b_{rand}^k(j,m,l) \right\|} \tag{11}$$

Where, step is the step size of a population individual at a time, $\varphi_i(j,m,l)$ is the chemotaxis direction, $b^k_i(j,m,l)$ is the current individual, $b^k_{rand}(j,m,l)$ is the random individual within the neighborhood, $\|\cdot\|$ is the hamming distance.

After performing a chemotaxis operator, namely, $b'_i(k)_{t+1} = b_i(k)_{t+1} = T_c^B(b_i(k)_t)$. If the fitness value of the population individual is not improved, namely, $f(b_i(k)_{t+1}) > f(b_i(k)_t)$, the population jumps out of(from?) the loop. If the fitness value of the population individual is improved, namely, $f(b_i(k)_{t+1}) < f(b_i(k)_t)$, the population individual walks forward along the same direction until that the fitness value of the population individual is not improved or the number of chemotaxis operator is the maximum.

3.2 Reproduction operator T_r^B

After chemotaxis operator, the population individual begins to reproduct following the principle of 'superior bad discard, survival of the fittest'. On the basis of fitness value of the population individual, half of the worse population individuals die, while another half of the better one split into two individuals. The reproduction operator is defined as:

$$B''(k) = T_r^B(B'(k)) = [b_1''(k)\ \ b_2''(k)\cdots\ b_n''(k)]^T \tag{12}$$

$\forall i \in [1,n]$, $\forall j \in [1,n]$, $i \neq j$, $b_i''(k) = T_r^B(b_i'(k))$ .namely, $b''_{i^{bad}}(k) = b'_{j^{good}}(k)$, $b''_{i^{good}}(k) = b'_{j^{good}}(k)$.

3.3 Elimination-dispersal operator T_e^B

The chemotaxis operator can ensure the local search ability of the population individual, the reproduction operator can accelerate the search speed of the population individual. But, for complex optimization problems, chemotaxis operator and reproduction operator can't avoid that the population individual falls into local minimum. The elimination-dispersal operator can strengthen the global optimization ability to BFA. After the reproduction operator, the population individual is migrated to any place in the search space in the probability of p_e. The elimination-dispersal operator is defined as:

$$B'''(k) = T_e^B(B''(k)) = [b_1'''(k)\ \ b_2'''(k)\cdots\ b_n'''(k)]^T \tag{13}$$

$\forall i \in [1,n]$, $b_i'''(k) = T_e^B(b_i''(k))$. According to p_e, $b_i''(k)$ goes to die, but $b_i'''(k) = b_i^{rand}(k)$.

IV. Clonal Selection Algorithm Based on Bacterial Foraging

In order to further improve the ability of global path planning of coal mine rescue robot in the complex environment, a bacterial foraging algorithm-based polyclonal selection algorithm is proposed. The bacterial foraging algorithm is introduced into the polyclonal selection algorithm to solve the convergence phenomenon which often occurs in the basic PSA at the late of the optimization causing the algorithm to fall into local minima. The chemotaxis operator makes the population individuals move in the direction of the target which can accelerate convergence. The reproduction operator increases search speed and makes the individuals have similar convergence speed, which can increase the parallelism of the algorithm and jump out of local minimum

value. After clonal selection algorithm, the elimination-dispersal operator can enhance population diversity and avoid falling into local optimal solution.

4.1 Detailed steps of the algorithm

Step1: Parameter initialization.
Step2: Population initialization: $G(k)$.
Step3: Genetic algebra initialization: k=1.
Step4: Chemotaxis operator:$G_{Bc}(k) = T_c^B(G(k))$.
Step5: Reproduction operator: $G_{Br}(k) = T_r^B(G_{Bc}(k))$.
Step6: Clonal selection algorithm:
Step6.1: Clonal operation: $G_{Cc}(k) = T_c^C(G_{Br}(k))$;
Step6.2: Immune gene operation: $G_{Cg}(k) = T_g^C(G_{Cc}(k))$;
Step6.3: Clonal selection operation: $G_{Cs}(k) = T_s^C(G_{Cg}(k))$.
Step7: Elimination-dispersal operator: $G_{Be}(k) = T_e^B(G_{Cs}(k))$.
Step8: $G(k) = G_{Be}(k)$.
Step9:$k \leftarrow k+1$, return to step4 while $k \leq k_{max}$.

4.2 Optimization and Analysis of the traveling salesman problem

In order to verify the optimization performance of the BFA-PSA, the traveling salesman problem(TSP) [19]is tested using Matlab7.01 on PIV 2.99 GHz 2 GB memory computer, and the test results are compared with those of GA and CSA. Considering the randomness of three intelligent algorithms , each simulation is tested independently for 50 times.

Table 1 gives the TSP optimization results of three optimization algorithms. From the table, it can be seen that minimum distance, maximum distance and average distance of the BFA-PSA in the six TSP optimizations are the least,which shows the strong optimization ability of the BFA-PSA. The minimum convergence generation, maximum convergence generation and average convergence generation Maximum show the quick convergence speed of the BFA-PSA. From the results, we can see that both the optimization ability and convergence speed of the BFA-PSA are the best, while that of the GA are the worst.

Table 1 TSP optimization results of GA, CSA and BFA

Number of the city	Algorithm name	Minimum distance	Maximum distance	Average distance	Minimum convergence generation	Maximum convergence generation	Average convergence generation
	GA	73.9876	83.184	75.1687	28	910	207.18
16	CSA	73.9876	79.0614	74.6442	11	52	28.44
	BFA-PSA	73.9876	78.8341	74.6137	6	11	9.14
	GA	9138.984	10880.34	9807.131	142	993	379.38
29	CSA	9076.9829	10690.75	9563.436	68	165	101.6
	BFA-PSA	9074.148	10353.72	9466.792	28	56	38.98
	GA	16465.037	19414.30	17372.03	163	986	379.68
31	CSA	16296.43	18585.09	17181.02	80	180	124.26
	BFA-PSA	16218.239	18222.09	16867.15	31	51	42.28
	GA	780.1952	891.8112	833.6517	953	1000	984.22
101	CSA	686.1471	761.3026	720.5195	842	1000	963.76
	BFA-PSA	674.81	738.7152	711.0682	367	998	457.82
	GA	9251.52	11445.62	11445.62	975	1000	992.76
130	CSA	6639.21	7605.88	7205.06	960	1000	992.58
	BFA-PSA	6405.19	7433.49	6843.01	567	910	712.26
	GA	10400.675	11961.07	11163.50	989	1000	997.28
225	CSA	7548.9597	8529.520	8062.314	993	1000	998
	BFA-PSA	4630.1311	5116.747	4890.804	992	1000	998.5

Fig.1 shows the path planning for 130 cities of GA,CSA and BFA-PSA. From the figure, it can be seen that compared with GA, CSA, the path planning for 130 cities of BFA-PSA is the most reasonable and the distance is the minimum, which further verifies optimization ability of the BFA-PSA is the strongest.

Fig.2 shows the evolutionary curves of GA, CSA and BFA-PSA during the path planning for 130 cities. From the figure, it can be seen that the convergence speed of BFA-PSA is the fastest, while the convergence speed of GA is the slowest. The global optimization ability of BFA-PSA is the strongest, while the global optimization ability of GA is the weakest. The figure further verifies the effectiveness of the BFA-PSA.

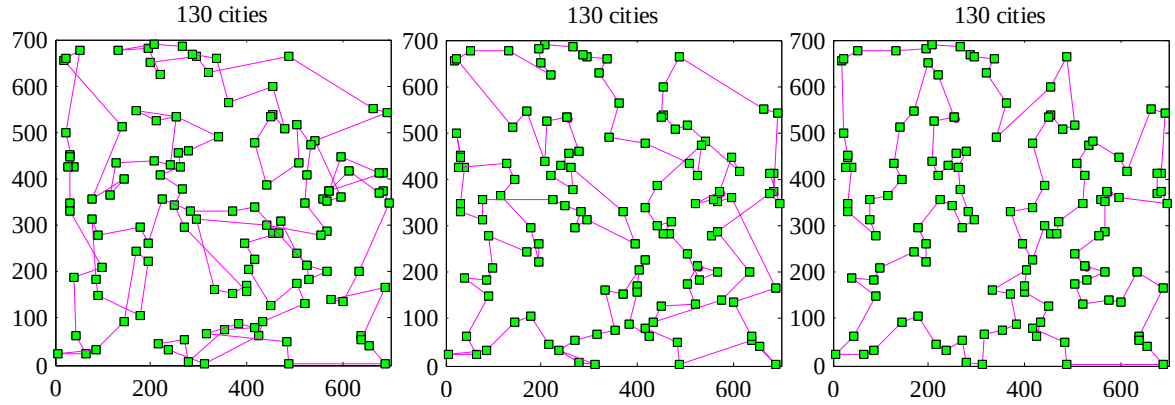

(a) Path planning of GA (b) Path planning of CSA (c) Path planning of BFA-PSA

Fig.1 Path planning for 130 cities of GA,CSA and BFA-PSA

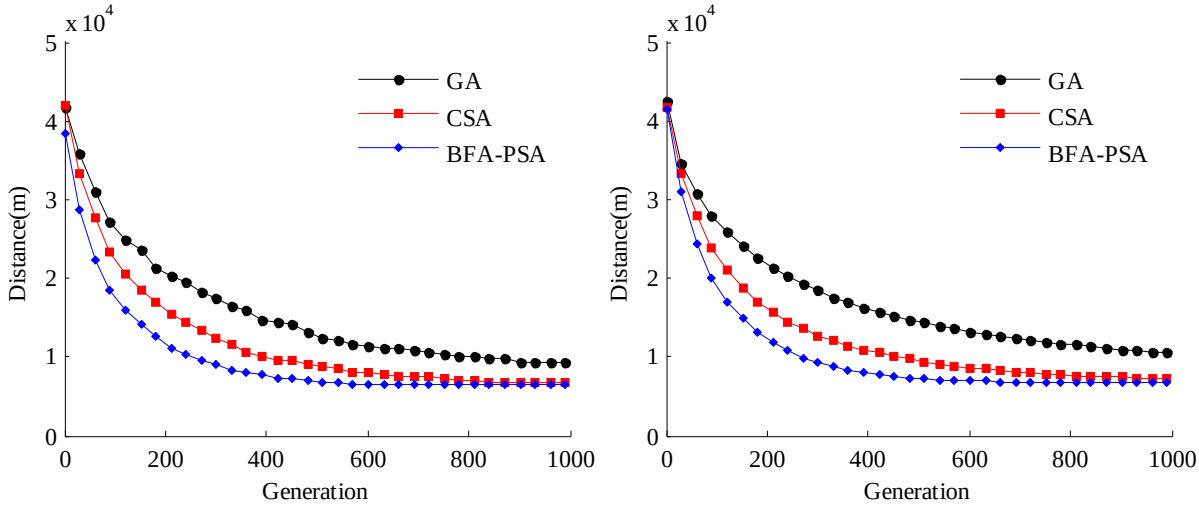

(a) The optimal solution (b) The average solution

Fig.2 Average evolution curves of the path planning for 130 cities

V. Optimization of Path Planning for Coal Mine Rescue Robot

5.1 Environmental modeling

The environmental modeling[20] is an important part of the robot path planning. This paper uses the grid method to model, and the data employs direct encoding.

XY is a limited motion area in the plane of two-dimensional, and there are a finite number of static obstacles Obs_i (i = 1, 2, ⋯ , n) in the area. According to the actual size of the robot and the security requirement, this paper does swelling processes to the obstacles, namely, a grid is occupied by an obstacle, no matter how big the occupied area is, the grid is seen as a obstacle. In addition, the robot is seen as a particle on the premise that the results are not affected. Fig.3 shows a grid sequence, and the black in the figure shows the obstacle.

x_{max} is the maximum of the grid in the direction of X, y_{max} is the maximum of the grid in the direction of Y, l is the side length of the single grid, and the step of the robot is l, so the grid number of each row is N_x, the grid number of each column is N_y, namely, $N_x = x_{max} / l$, $N_y = y_{max} / l$.

v is the any grid in the plane of XY, V is the sum of the grid in the plane of XY, $v(x,y)$ is the any grid that its center coordinates are x and y, so $v \in V$. N={1,2,⋯,n} is the grid serial number, $v_i(x_i,y_i)$ shows the grid that its serial number is i ($i \in N$). The mapping relationship of the serial number i and (x_i,y_i) which is the coordinates of v_i is can be described as follows:

$$\begin{cases} x_i = \mathrm{mod}((i-1), N_x) \times l + \dfrac{l}{2} \\ y_i = \mathrm{floor}((i-1)/N_y) \times l + \dfrac{l}{2} \end{cases} \quad (14)$$

Where, mod(·) is the modulo operation, floor(·) is the down integral function.

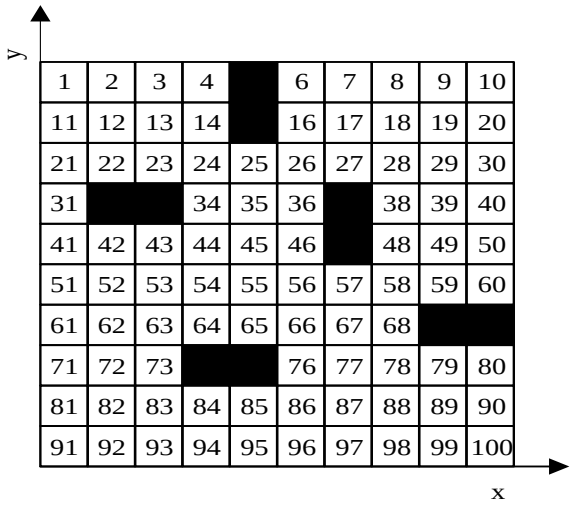

Fig.3 Grid sequence diagram

5.2 Initialization of the population

Taking an example of a 10*10 grid, the starting point *S* is the grid that the sequence number is 1, and the end point *E* is the grid that the sequence number is 100. There are feasible points of one to eight from some point to the next point. The generation process of the population can be described as follows:

Step1: The robot starts from the starting point *S*.

Step2: Determine all the next points that are feasible.

Step3: Calculate the distance from the feasible points to the end and choose the next point in the form of roulette.

Step4: Determine whether the robot reaches the end *E* . If the robot reaches the end, a population individual is generated . Then, start to generate the next individual until the population is generated . If the robot does not reach the end, return to Step2.

5.3 Path planning

In order to further verify the validity of the BFA-PSA in the practical application, the BFA-PSA is applied to the optimization of the path planning for coal mine rescue robot. BFA-PSA is tested using Matlab7.01 on PIV 2.99 GHz 2 GB memory computer in six different environment, and the test results are compared with the test results of GA and CSA. Considering the randomness of three intelligent algorithms, each simulation is tested independently for 50 times.

Table 2 Path planning results of GA, CSA and BFA-PSA

Environment	Minimum distance			Maximum distance			Average distance			Stand deviation		
	GA	CSA	BFA-PSA	GA	CSA	BFA-PSA	GA	CSA	BFA-PSA	GA	CSA	BFA-PSA
1	36.97	32.72	30.38	128.4	51.21	37.79	59.02	33.69	31.64	9.257	1.006	0.545
2	40.87	36.14	28.62	104.9	59.69	51.45	66.78	37.67	31.22	13.07	3.049	2.393
3	39.79	29.21	28.63	105.0	59.70	48.28	62.83	38.04	32.86	6.700	5.166	5.165
4	39.62	33.55	32.38	99.74	58.52	47.69	60.34	40.62	36.82	9.779	3.610	1.738
5	35.97	30.55	30.40	95.08	57.11	47.45	58.11	34.97	33.20	8.884	4.736	0.926
6	34.38	31.56	29.21	92.25	55.11	54.52	58.21	35.75	33.23	9.675	4.267	4.035

Table 2 gives the path planning results of GA, CSA and BFA-PSA. From the minimum distance, maximum distance and average distance, it can be seen that the BFA-PSA has the strongest optimization ability. The stand deviation shows the good stability of BFA-PSA.

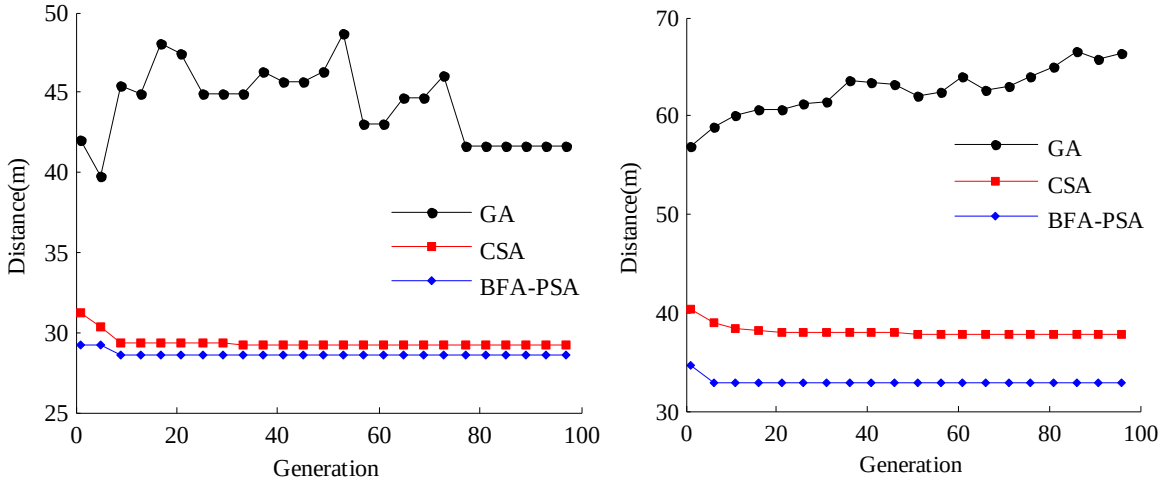

(a) The optimal solution (b) The average solution

Fig.5 Average evolution curves of the path planning for environment 3

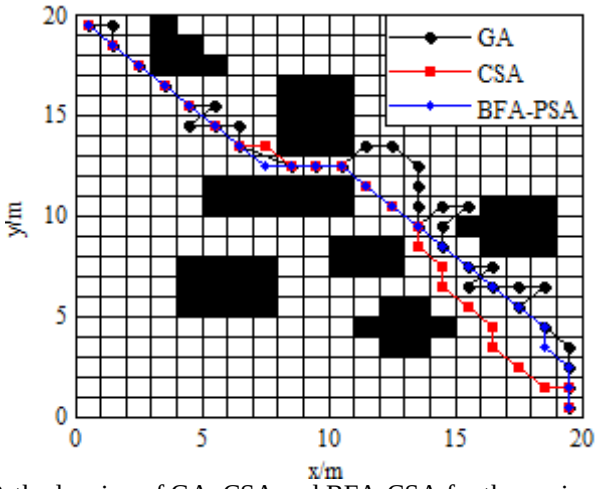

Fig.6 Path planning of GA, CSA and BFA-CSA for the environment 3

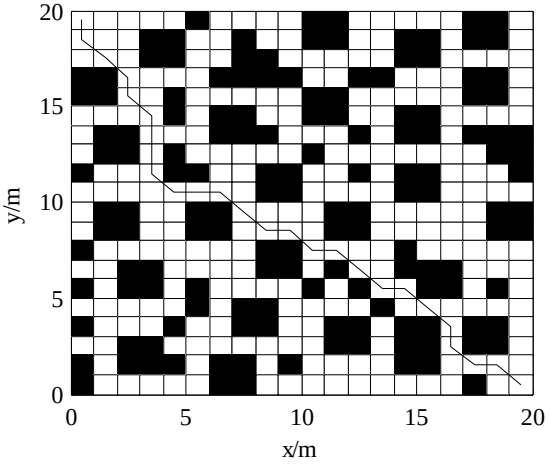

Fig.7 Path planning of BFA-CSA for the random environment

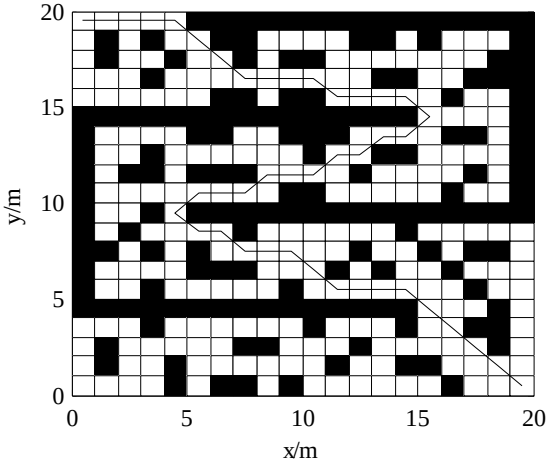

Fig.8 Path planning of BFA-CSA for the simulated mine roadway after a disaster

Fig.5 shows the evolutionary curves of GA, CSA and BFA-PSA during the path planning for environment 3. From the figure, it can be seen that the convergence speed of BFA-PSA is the fastest, the global optimization ability of BFA-PSA is the strongest. The figure further verifies the effectiveness of the BFA-PSA.

Fig.6 shows the path planning of GA, CSA and BFA-CSA for the environment 3. From the figure, it can be seen that the path planning of BFA-CSA is the best which shows the strong optimization ability of the BFA-PSA.

In order to prove the generality of the BFA-CSA, this paper uses the BFA-CSA to plan path in the random environment. Fig.7 shows the path planning of BFA-CSA for the random environment. From the figure, it can be seen that the robot can find the optimal path in a complex environment, which shows the strong robustness of the BFA-CSA.

Fig.8 shows the path planning of the BFA-CSA for the simulated mine roadway after a disaster. From the figure, it can be seen that the robot can find the optimal path to arrive at the scene of the disaster, which can strive for more time for mine rescue.

VI. Conclusion

In order to further improve the ability of global path planning of coal mine rescue robot in the complex environment, a bacterial foraging algorithm-based polyclonal selection algorithm (BFA-PSA) is proposed. The chemotaxis operator, reproduction operator and elimination-dispersal operator are added in the polyclonal selection algorithm to improve the convergence speed and retain the diversity of the population. The optimization results of TSP and path planning in six different environment show the fast convergence speed and strong optimization ability of the BFA-PSA, and the optimization results of path planning in the random environment and the simulated mine roadway after a disaster show that the robot can find the optimal path in a complex environment and strive for more time for mine rescue.

Acknowledgements

The project is supported by the National High Technology Research and Development Program of China (863 Program) (Grant No. 2012AA041504) and the Priority Academic Program Development of Jiangsu Higher Education Institutions.

References

[1] G.Q.Wang, H.S.Xu, K.R.Wang, Research status and development trend of coal mining robots, Coal Science and Technology, 42(2), 2014, 73-77.
[2] G.D.Sun, Y.T.Li, H.Zhu, Design of a new type of crawler travelling mechanism of coal mine rescue robot, Industry and Mine Automation, 41(6), 2015,21-25.
[3] J.R.Spofford, D.J.Anhalt, J.B.Herron, B.D.Lapin, Collaborative robotic team design and integration，International Society for Optics and Photonics, 2000,241-252.
[4] J.Y.Gao, X.S.Gao, J.G.Zhu, et al, Light Mobile Robot Power Common Technique Research, 2009 International Conference on Intelligent Human-Machine Systems and Cybernetics, 2009, 90-94.
[5] C.S. Moo, K.S.Ng, Y.C.Hsieh, Parallel Operation of Battery Power Modules, Sixth International Conference on Power Electronics and Drive Systems, 2005,983-988.
[6] Y.W.Li, S.R.Ge, H.Zhu, et al, Obstacle-surmounting mechanism and capability of four-track robot with two swing arms, Robot, 32(2),2010, 157-165.
[7] Y.W.Li, S.R.Ge, H.Zhu, Deduction of the rocker-type track suspension configurations and their applications to coal mine rescue robots, Robot, 32(1),2010, 25-33.
[8] Y.W.Li, S.R.Ge, H.Zhu, Mobile Platform of a Rocker-type W-shaped Track Robot, Key Engineering Materials, 419-420,2010, 609-612.
[9] Y.W.Li, S.R.Ge, H.Zhu, Mobile Platform of Rocker-Type Coal Mine Rescue Robot, Mining Science and Technology, 20 (3),2010, 66-471.
[10] L.Zhu, J.Z.Fan, J.Zhao, et al, Global path planning and local obstacle avoidance of searching robot in mine disasters based on grid method, Journal of Central South University (Science and Technology), 42(11),2011, 3421-3428.
[11] D.Q.Zhu, M.C.Yan, Survey on technology of mobile robot path planning, Control and Decision, 25(7),2010, 961-967.
[12] Z.Z.Yu, J.H.Yan, J.Zhao, et al, Mobile robot path planning based on improved artificial potential field method, Journal of Harbin Institute of Technology, 43(1), 2011, 50-55.
[13] J.J.Wang, K.Cao, Path-planning for robot based on grid algorithm, Agricultural Equipment & Vehicle Engineering, 4, 2009, 14-17.
[14] Y.Song, Y.B.Li, C.Li, et al, Path planning methods of mobile robot based on neural network, Systems Engineering and Electronics, 30(2), 2008,316-319.
[15] Z.B.Su, J.L.Lu, A study on the path planning of mobile robot with the fuzzy logic method, Transactions of Beijing Institute of Technology, 23(3), 2003, 290-293.
[16] X.Chen, G.Z.Tan, B.Jiang, Real-time optimal path planning for mobile robots based on immune genetic algorithm, Journal of Central South University (Science and Technology), 39(3), 2008, 577-583.
[17] Y.Shen, M.X.Yuan, Q.Wang, Virus evolutionary immune clonal algorithm for optimization of manipulator, Computer Engineering and Applications,47(31), 2011, 224-226.
[18] Y.L.Zhou, Research and application on bacteria foraging optimization algorithm, Computer Engineering and Applications, 46(20), 2010, 16-21.
[19] M.Li, L.Wu, K.B.Zhang, Comparative study of several algorithms for traveling salesman problem, Journal of Chongqing University of Posts and Telecommunications (Natural Science Edition), 20(5), 2008, 624-626.
[20] Y.Shen, M.X.Yuan, Y.F.Bu, Study on adaptive planning strategy using ant colony algorithm based on predictive learning, Control and Decision Conference, 2009. CCDC'09. Chinese. IEEE, 2009: 3030-3035.